

Convective lofting links Indian Ocean air pollution to paradoxical South Atlantic ozone maxima

R. B. Chatfield,¹ H. Guan,^{1,2} A. M. Thompson,³ and J. C. Witte^{3,4}

Received 17 October 2003; revised 3 December 2003; accepted 4 February 2004; published 16 March 2004.

[1] We describe a broad resolution of the “Atlantic Paradox” concerning the seasonal and geographic distribution of tropical tropospheric ozone. We highlight periods of significant maximum tropospheric O₃ for Jan.–April, 1999, exploiting satellite estimates and SHADOZ (Southern Hemisphere Additional Ozonesondes). Trajectory analyses connecting sondes and Total Tropospheric Ozone (TTO) maps suggest a complex influence from the Indian Ocean: beginning with mixed combustion sources, then low level transport, cumulonimbus venting, possible stratospheric input, and finally high-level transport to the west, with possible mixing over Africa. For the Jan.–March highest column-O₃ periods in the Atlantic, distinct sounding peaks trace to specific NO sources, especially lightning, while in the same episodes, recurring every 20–50 days, more diffuse buildups of Indian-to-Atlantic pollution make important contributions. *INDEX TERMS:*

0322 Atmospheric Composition and Structure: Constituent sources and sinks; 0365 Atmospheric Composition and Structure: Troposphere—composition and chemistry; 3374 Meteorology and Atmospheric Dynamics: Tropical meteorology; 9340 Information Related to Geographic Region: Indian Ocean.

Citation: Chatfield, R. B., H. Guan, A. M. Thompson, and J. C. Witte (2004), Convective lofting links Indian Ocean air pollution to paradoxical South Atlantic ozone maxima, *Geophys. Res. Lett.*, 31, L06103, doi:10.1029/2003GL018866.

1. The Tropical Atlantic Paradox

[2] From the time that unexpectedly high O₃ was first discovered over the Equatorial Atlantic [Logan and Kirchhoff, 1986; Fishman *et al.*, 1990], biomass burning and smog over the adjacent continents have seemed mainly responsible [Dickerson, 1984; Crutzen *et al.*, 1985; Chatfield and Delany, 1990]. Additional O₃ data available from aircraft, soundings and satellite, make it clear that the mechanisms controlling O₃ distributions in this region are more complex. There is evidence for interhemispheric transport, especially from the end-of-dry-season or “burning” hemisphere (local winter-spring) towards the end-of-wet season hemisphere. [Jonquière *et al.*, 1998; Thompson *et al.*, 2000; Edwards *et al.*, 2003; Jenkins *et al.*, 2003; Peters *et al.*, 2002]. The striking appearance of a maximum in South Atlantic O₃ while northern Africa has maximum

fire activity constitutes a “tropical Atlantic paradox” [Thompson *et al.*, 2000]. Explanations include the seasonality of interhemispheric transport, regional subsidence and lightning [Martin *et al.*, 2002; Edwards *et al.*, 2003; Jenkins *et al.*, 2003]. Recently Martin *et al.* [2002] and Peters *et al.* [2002] have noted the difficulty of quantitative event simulations compared to non-specific seasonal descriptions. They also illustrate the inability of 3-D models to simulate suitably narrow upper tropospheric plumes.

[3] We investigate a period with exceptional O₃ sounding coverage over the tropical Atlantic, Africa and the Indian Ocean region, early 1999, using the SHADOZ network [Thompson *et al.*, 2003]. We use these data to examine possible linkages between O₃ over the Atlantic and Indian Oceans for the winter “paradox” period.

2. Data and Methods

[4] Ozone soundings are taken from the SHADOZ [Thompson *et al.*, 2003] data archives. Satellite tropospheric O₃ column data, time-averaged to 5-days, are based on the modified-residual method [Thompson and Hudson, 1999, <http://croc.gsfc.nasa.gov/shadoz>]. Generally, these resemble other TOMS-based tropospheric O₃ column estimates [Fishman *et al.*, 1990], and are increasingly sensitive to O₃ above 600 mb. Although there are questions about details of TOMS-based tropospheric O₃ retrievals over Africa and the Atlantic [Martin *et al.*, 2002], the modified-residual data agree quite well with the sonde record for early 1999. Tapered (5-day) running averages were used to smooth TTO and fill in gaps.

[5] The Goddard kinematic trajectory model [Schoeberl and Newman, 1995] was employed with gridded analyses at resolution 3.75 × 2.5, from the UKMO, and 2.5 × 2.5, from NCEP. UKMO winds were preferred for regions with substantial vertical motion, for they had better vertical velocities. Lightning sources for the upper tropospheric source of O₃-precursor NO_x were taken from the Lightning Imaging Sensor (LIS) [Christian *et al.*, 1992]. 5-day averages of LIS allowed us some fill-in of data gaps and averaging over the diel cycle of lightning; this limited sampling adequately defines patterns on a regional basis when compared to longer averages. VIRS (Visible Infrared Radiation Sensor) estimates, a monthly average product based on hot pixels, is indicative of open-field or open-forest burning. [Giglio and Kendall, http://daac.gsfc.nasa.gov/CAMPAIGN_DOCS/hydrology/TRMM_VIRS_Fire.shtml] We also considered 1997 monthly mean TOMS Aerosol Index (TAI) to define larger regions affected by burning. [<http://toms.gsfc.nasa.gov/aerosols/aerosols.html>]. These indicate near-surface sources of NO and organics, and also O₃. Low outgoing longwave radiation (OLR)

¹NASA Ames Research Center, USA.

²BAER Inst., USA.

³NASA Goddard Research Center, USA.

⁴SSAI, USA.

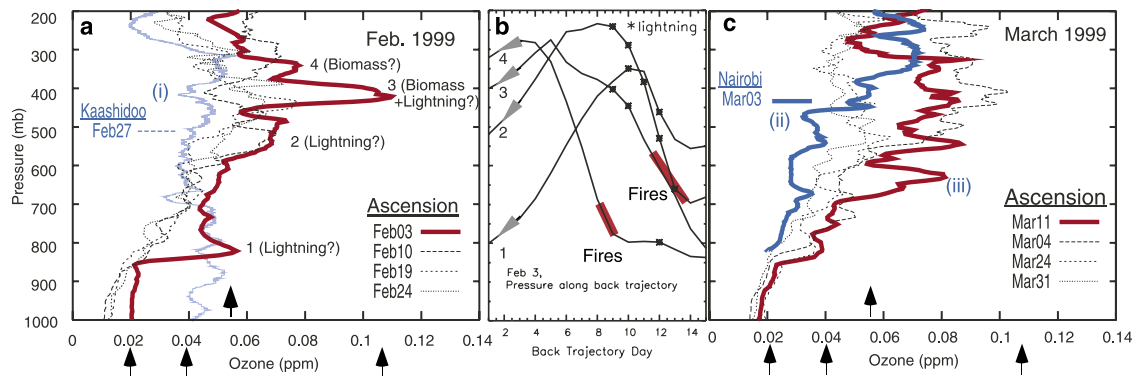


Figure 1. SHADOZ sondes launched during February–March, 1999, with analysis. (a) February Ascension sondes (black, red), for red sounding, suggested origins: see Section 3.1. Also: light blue trace marked (i): Kaashidoo, Indian Ocean, Feb. 27; Section 3.2. (b) Vertical motions associated with UKMO back trajectories from indicated levels at Ascension island. * indicates substantial lightning activity noted along the trajectory. Also indicated are biomass burning influences. (c) Soundings indicating peaks and background in March 1999. Ascension (black; red, marked (iii)). Nairobi (blue, marked (ii)). Short vertical arrows illustrate “background” O₃ attributions: see Section 3.2.

allowed us to locate regions with high convective cloud tops.

3. Results. Ozone Peaks, Background, and Transport

[6] Analysis of O₃ over Ascension Island, typical of the south tropical Atlantic, shows two important features: (1) Peaks of pollution in soundings, for which air-parcel trajectories and ozone precursor source proxies allow attribution (Section 3.1); (2) broad changes in apparent “background” O₃ that are further examined with satellite ozone, trajectories and ancillary data (Section 3.2).

3.1. Ozone Peaks at Ascension and Atlantic Subsidence

[7] Four ozonesondes launched over Ascension Island (8S, 15W) during February 1999 (Figure 1a) show time-varying and distinct layers above 800 mb. Consider an obvious question: which processes are responsible for the distinct peaks in the February O₃ profiles? The highlighted sounding for February 3 is used for specific analysis and

four peaks are labeled. Figure 1b shows vertical transport associated with the trajectories. Trajectories for Peaks 1, 2, 3 experienced strong subsidence for several days prior to the endpoint. Figure 1b also shows exposure to lightning (within 0–300 km of detected LIS “strikes”). In the same way, we marked regions of exposure to lofting of biomass burning emissions (deep clouds signaled by low OLR, high VIRS and TAI below). Figure 2 (upper) provides a map of the trajectories keyed to Figure 1b, with locations of the LIS lightning and VIRS fire data for February 3. The blue contour (lower panel, with TTO maps) indicates subsidence >0.05 Pa/s and high O₃ over a large region near Ascension.

[8] The lower tropospheric peaks (1, 2) in the February 3 sounding seem to derive from lightning-produced ozone which descended several km over ten days. In general, regions of the sounding without peaks did not pass over lightning or burning areas. Peak 3 originated from the Sahel of North Africa where biomass burning persisted into February. The strong O₃ peak 3 may well have passed for several thousands of km over a region with biomass burning emissions blowing southward from west Africa to a coastal

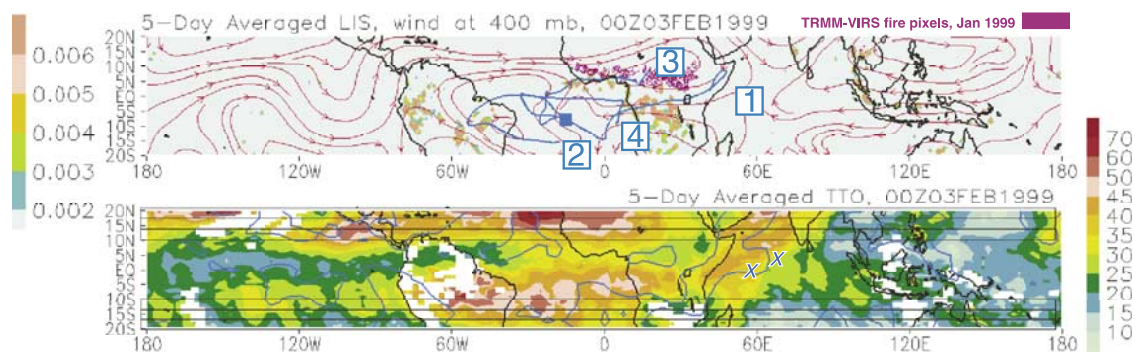


Figure 2. (Top) Sample back trajectories for plumes 1, 2, 3, and 4 sampled at Ascension February 3, 1999, overlaid on LIS and 400-mb wind field maps. January 1999 biomass burning map is overlaid (purple). (Bottom) TTO map contains blue curves indicating 0.05 Pa s⁻¹ vertical velocity contours at 850 mb. Horizontal bars at 10–20 latitude indicate where TTO loses accuracy. Some diagonal striping seen in 5-day averaged TTO maps disappears with time averaging.

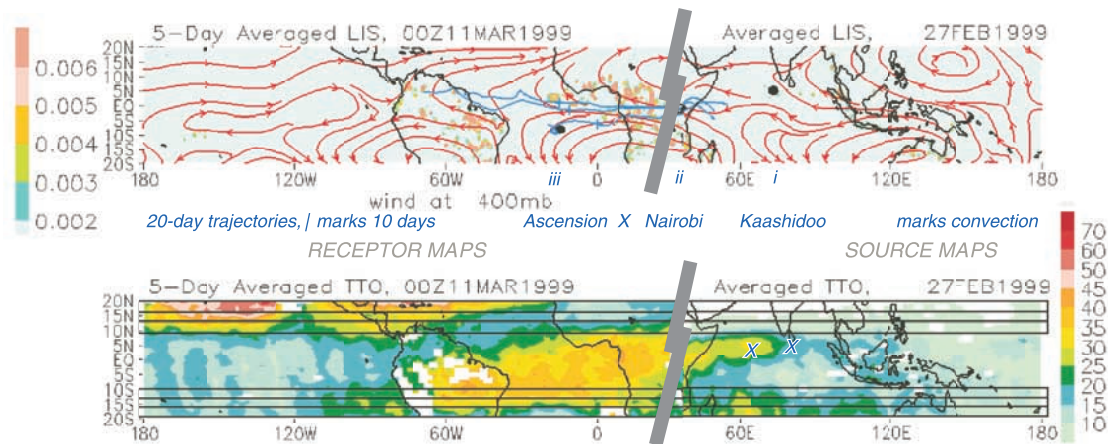


Figure 3. Analysis of LIS and TTO similar to Figure 2 but for receptor (left) and source (right) regions of long-range transport, analyses separated by gray bars. Note remarkable constancy of westward 400-mb Equatorial winds between 27 February (venting period in Indian Ocean) and 11 March (sonde O₃) at Ascension. Trajectories on both panels show a cluster of upper-air trajectories forward from a region of high cloud that extended westward into the Indian Ocean, starting 27 February. X marks convection on the 25th and 27th.

region with some lightning. It is known that upper tropospheric NO from lightning can interact with ROO radicals from lofted pyrogenic emissions to produce O₃ at the rate of 10 ppbv/day or more [Thompson *et al.*, 1996]. Peak 2 at 550 mb may also have contributions from Brazilian pollution. Many of the daily TTO maps for the January–March 1999 period (not shown) are similar. Air circling into or passing through regions of strong Atlantic subsidence tend to have the thickest column-integrated ozone when compared to the equatorial average. These four specific peaks illustrate in one sounding previously described mechanisms for “paradoxical” O₃ enhancement in the tropical Atlantic, but there seems to be an additional contribution we now describe.

3.2. Distant Sources of Broader, Mid-Tropospheric Elevated Ozone

[9] Figure 1 shows a difference between “background” ozone underlying the peaks when the February (Figure 1a) and March features (Figure 1c) are compared. The SHADOZ sondes from Samoa (14S, 171W) or Galapagos (1S, 90W) in the Pacific, have about ~20 ppbv above 700 mb Thompson *et al.* [2003]. Small arrows in Figure 1 indicate the “global background” of 20 ppbv as inferred from ozone in these regions. Also indicated are a minimum seasonal background of around 40 ppb (see March 24 and March 31), an enhanced background of 55–60 ppbv. (see February sondes and March 4 and 11), and peak plume O₃ (>105 ppbv) seen on the February 3 profile. It appears that such elevated background O₃ can account for about half the Atlantic column burden.

[10] What are the origins of the broad increases in background O₃ between 850 and 250 mb seen, for example, in February 3 and March 11? In addition to merging of plumes and subsidence (discussed in Section 3.1), we illustrate a long-distance process that includes the Indian Ocean and acts intermittently to enhance column O₃ to its

highest values. TTO maps and O₃ soundings over Ascension suggest that total tropospheric O₃ decreased in mid-February but then increased again in the period covered by the March 4–11 soundings. Focus on the O₃ increase from 700 to 300 mb in the March 11 sounding (Figure 1c), an increase which is corroborated by the TOMS TTO for the broad area around Ascension (also for the several-week period prior to the sounding). Figure 3 shows in one display two different periods, the arrival at Ascension (left: March 11) and a period associated with O₃ origins (right: February 27), in the central Indian Ocean. A stream of Indian Ocean TTO (in the well-sensed upper troposphere) appeared in the suddenly and in isolation during 24–25 February and spread westward with strong extra O₃ input on February 27. The additional O₃ coincided with deep clouds on both days (“X” in Figure 3). Zachariasse *et al.* [2001] found stratospheric O₃ in the uppermost troposphere shortly thereafter. INDOEX studies have revealed a substantial region of smog pollution recurrently affecting the lower troposphere [Ramanathan *et al.*, 2001]. The Rasch *et al.* [2001] simulations of hydrophilic carbon aerosol portray lower tropospheric smog during this period.

[11] A profile view of this elevated O₃ in lower and upper troposphere was captured in the INDOEX sondes at Kaashidoo (5°N, 73°E), February 25 (light blue curve in Figure 1a). Analysis of moisture in the sounding could not rule out either convective lifting of polluted air or a limited stratospheric influence. (Zachariasse *et al.* [2001] found the latter influence more evident later in March and our TTO map are consistent with this.) Using daily OLR maps as a guide we started forward trajectories from the approximate location of the cloud output region, ~250 mb on February 24 and 27. Figure 3 shows three trajectories of a cluster from February 27, with direct flow across Africa, corroborated by a ribbon of high TTO (35 DU) progressing across central Africa each day similar to those on the days

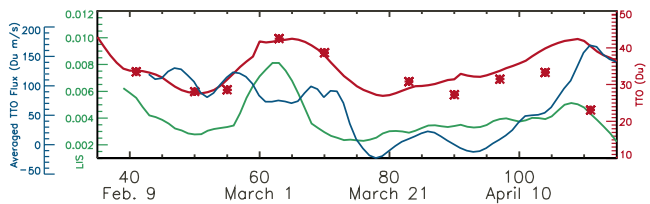


Figure 4. Time series relating tropospheric O₃ in the Central Atlantic to lightning and O₃ inflow from the Indian Ocean. Green: approximate LIS lightning flash incidence (s⁻¹) over Central Africa (10–20°E., 6.5°S to 1.5°N) — shifted 7 da, approximating transport time. Blue: A measure of the westward flux of O₃ estimated using daily TTO values and averaged winds between 300–600 mb along a “wall” on the West Coast of Africa—shifted 11 da. Red: TTO O₃ at Ascension Island: sondes (*) mostly agree well.

shown. Africa is a region of mixing due to deep continental boundary layers, effects of steep topography, and energetic vertical cumulonimbus convection (high LIS values over central Africa, Figures 2 and 3).

[12] Clusters of 7-day backward trajectories from Ascension, March 3, (not shown) and clusters of forward trajectories from the cloud-venting regions provide similar results. UKMO and NCEP winds give consistent results. However, paths are not all so directly east-to-west as Figure 3 suggests. TTO maps show such a wide region of O₃-laden air crosses a broad region of central Africa during the transport period. Direct evidence for cross-African O₃ transit is shown at a midway point. At the correct altitude a Nairobi sonde (March 3, Figure 1c) shows a buildup to 65–70 ppbv O₃ between 275–475 mb. Based on the integral ozone observed in the Nairobi and Ascension sondes, we estimate that up to 45% ± 10% of ozone above regional background at Ascension is attributable to cross-African transport from the Indian Ocean region in these situations.

[13] How typical is this behavior? This view of Asian pollution combining with some fresh input is corroborated by a time-series study of O₃ and processes that increase it during early 1999. Figure 4 shows time series of TTO and sonde O₃ at Ascension, LIS lightning in central Africa, and a simple estimate of the westward flux of O₃. The estimate was constructed by multiplying TTO O₃ column amounts by averaged winds in a rectangular area oriented as an “entrance door” to Central Africa: 5°S to 10°N along a meridian at 40°E, and 300 to 600 mb in the vertical. Considering the variability of wind speeds and pathways, the delayed reaction of the TTO at Ascension is remarkably correlated to an appropriate sum of these two quantities, with constant eyeball-fit time delays that match well with averaged transport times. These TTO maxima correlate with periods of enhanced “background” seen in the February 3, March 4, and March 11 soundings at Ascension. For the case of Figure 2, there was appropriate convection 11 days prior at locations marked “X”, and westward winds for inter-ocean transport, but there is no TTO data to complete the analysis. The periods of maximum TTO recur irregularly, every 20–50 days, suggesting intraseasonal tropical variability. Zachariasse et al. [2001] found differing March weather and O₃ for 1998–1999; we expect intraseasonal (e.g., 20–50 da, using plots of Ascension TTO vs.

time for 1998 and 1999) variations complicate interannual comparisons. The pollution phenomenon seems to occur other years; e.g., a similar swath of Indian Ocean to Atlantic Ocean transport around 8–17 March, 1998. This pattern of eastward transport from the Indian Ocean also seems to appear outside late winter, as Krishnamurti et al. [1996] first noted. We expect sources and wind patterns to vary with season, so, while we expect some relation of this transport pattern to the Madden-Julian oscillation, that relation requires investigation beyond this report.

4. Conclusions

[14] For our analysis of the late-winter period, plumes of O₃ in the South Atlantic can be related to sources on nearby continents, particularly lofting of biomass burning emissions and lightning. Subsidence around, and to the south of Ascension Island, tends to enhance the O₃ column as high O₃ fills in from above. Characteristic higher background O₃ profiles and higher TTO derive significantly from long range transport from Indian Ocean pollution. This long-distance O₃ apparently has a source in multi-source pollution NO_x and organics emissions which flow from South Asia during the winter months, and perhaps some stratospheric input. The brown-cloud process is well described for 1999 in the INDOEX papers [Lelieveld et al., 2001; Ramanathan et al., 2001]. In summary, the ozone paradox is explained by accumulation (subsidence) acting on both plumes and thicker layers, layers which may travel 10,000 km eastward under certain recurrent meteorological conditions.

[15] **Acknowledgments.** Thanks to NASA’s ACPMAP Program, to W. Peters, J. Olson, K. Pickering, M. Schoeberl and P. Newman.

References

- Chatfield, R. B., and A. C. Delany (1990), Convection links biomass burning to increased tropical ozone: However, models will tend to overpredict O₃, *J. Geophys. Res.*, 95(D11), 18,473–18,488.
- Christian, H. J., R. J. Blakeslee, and S. J. Goodman (1992), Lightning imaging sensor (LIS) for the earth observing system, NASA TM-4350, Center for Aerospace Information, P.O. Box 8757, Baltimore Washington International Airport, Baltimore, MD 21240.
- Crutzen, P. J., et al. (1985), Tropospheric chemical composition measurements in Brazil during the dry season, *J. Atmos. Chem.*, 2, 233–256.
- Dickerson, R. R. (1984), Measurements of reactive compounds in the free troposphere, *Atmos. Environ.*, 18, 2585–2593.
- Edwards, D. P., et al. (2003), Tropospheric ozone over the tropical Atlantic: A satellite perspective, *J. Geophys. Res.*, 108(D8), 4237, doi:10.1029/2002JD002927.
- Fishman, J., C. E. Watson, J. C. Larsen, and J. A. Logan (1990), The distribution of tropospheric ozone determined from satellite data, *J. Geophys. Res.*, 95(D4), 3599–3617.
- Jenkins, G. S., J.-H. Ryu, A. M. Thompson, and J. C. Witte (2003), Linking Horizontal and vertical transport of biomass fire emissions to the tropical Atlantic Ozone Paradox during the Northern hemisphere winter season, II. 1998–1999, *J. Geophys. Res.*, 108(D23), 4745, doi:10.1029/2002JD003297.
- Jonquière, I., A. Marengo, A. Maalej, and F. Rohrer (1998), Study of ozone formation and transatlantic transport from biomass burning emissions over West Africa during the airborne Tropospheric Ozone Campaigns TROPOZ I and TROPOZ II, *J. Geophys. Res.*, 103(D15), 19,059–19,073.
- Krishnamurti, T. N., et al. (1996), Passive tracer transport relevant to the TRACE-A experiment, *J. Geophys. Res.*, 101(D19), 23,889–23,907.
- Lelieveld, J., et al. (2001), The Indian Ocean Experiment: Widespread air pollution from South and Southeast Asia, *Science*, 291, 1031–1036.
- Logan, J. A., and V. W. J. H. Kirchhoff (1986), Seasonal-variations of tropospheric ozone at Natal, Brazil, *J. Geophys. Res.*, 91, 7875–7881.

- Martin, R. V., et al. (2002), Interpretation of TOMS observations of tropical tropospheric ozone with a global model and in situ observations, *J. Geophys. Res.*, *107*(D18), 4351, doi:10.1029/2001JD001480.
- Peters, W., M. Krol, F. Dentener, A.M. Thompson, and J. Lelieveld (2002), Chemistry-transport modeling of the satellite observed distribution of tropical tropospheric ozone, *Atmos. Chem. Phys.*, *2*, 103–120.
- Ramanathan, V., et al. (2001), The Indian Ocean Experiment: An integrated assessment of the climate forcing and effects of the great Indo-Asian haze, *J. Geophys. Res.*, *106*(D22), 28,371–28,399.
- Rasch, P. J., W. D. Collins, and B. E. Eaton (2001), Understanding the Indian Ocean Experiment (INDOEX) aerosol distributions with an aerosol assimilation, *J. Geophys. Res.*, *106*(D7), 7337–7355.
- Schoeberl, M. R., and P. A. Newman (1995), A multiple-level trajectory analysis of vortex filaments, *J. Geophys. Res.*, *100*(D12), 25,801–25,815.
- Thompson, A. M., and R. D. Hudson (1999), Tropical Tropospheric Ozone (TTO) maps from Nimbus-7 and Earth-Probe TOMS by the modified-residual method: Evaluation with sondes, ENSO signals and trends from Atlantic regional time series, *J. Geophys. Res.*, *104*(D21), 26,961–26,975.
- Thompson, A. M., et al. (1996), Where did tropospheric ozone over southern Africa and the tropical Atlantic come from in October 1992?, *J. Geophys. Res.*, *101*(D19), 23,251–24,278.
- Thompson, A. M., et al. (2000), A tropical Atlantic ozone paradox: Shipboard and satellite views of a tropospheric ozone maximum and wave-one in January–February 1999, *Geophys. Res. Lett.*, *27*(20), 3317–3320.
- Thompson, A. M., et al. (2003), Southern Hemisphere Additional Ozone-sondes (SHADOZ) 1998–2000 tropical ozone climatology. 2. Tropospheric ozone variability and the zonal wave-one, *J. Geophys. Res.*, *108*(D2), 8241, doi:10.1029/2002JD002241.
- Zachariasse, M., et al. (2001), Cross-tropopause and interhemispheric transports into the tropical free troposphere over the Indian Ocean, *J. Geophys. Res.*, *106*(D22), 28,441–28,452.

R. B. Chatfield and H. Guan, NASA Ames Research Center, USA. (chatfield@clio.arc.nasa.gov)

A. M. Thompson and J. C. Witte, NASA Goddard Research Center, USA.